Available online at www.sciencedirect.com
SCIENCE DIRECT®
Separation and Purification Technology 36 (2004) 215–228
Separation and Purification Technology
www.elsevier.com/locate/seppur

Gusev and Suter calculation of the diffusion coefficients of light gases in silicalite-1 membrane and silica-sodalite zeolite

Giorgio De Luca [a,*], Pluton Pullumbi [b], Giuseppe Barbieri [a], Angelo D. Famà [a], Paola Bernardo [a,c], Enrico Drioli [a,c]

[a] *CNR—Research Institute on Membrane Technology, Via Pietro Bucci, c/o University of Calabria Cubo 17/C, 87030 Rende CS, Italy*
[b] *Air Liquide, Centre de Recherche Claude Delorme, 1 Chemin de la Porte des Loges, B.P. 126, 78354 Les Loges-en-Josas Cedex, France*
[c] *Department of Chemical Engineering and Materials, c/o University of Calabria Cubo 17/C, Via Pietro Bucci, 87030 Rende CS, Italy*

Received 24 March 2003; received in revised form 2 July 2003; accepted 30 July 2003

Abstract

Transition-state theory (TST) as implemented by Gusev and Suter was applied to calculate the zero-loading-diffusion coefficients of 12 gases (He, Ne, Ar, Xe, H_2, N_2, O_2, CO_2, SF_6, CH_4, CF_4, and *i*-C_4H_{10}) in two different zeolites, silicalite-1 and silica-sodalite. Gusev–Suter (GS) model was and is widely and successfully used for polymeric matrixes. Therefore, the reliability of this method was studied for gas diffusion in silicalite-1 and silica-sodalite using CVFF_aug and CVFF force fields and two simulation cells. The results were compared with diffusion coefficients used to reproduce the permeance in a silicalite-1 membrane. Model limits were also tested comparing the H_2, He and Ne diffusion in silica-sodalite with previous calculations of classical and quantum TST. Gusev–Suter method systematically underestimates the average diffusion coefficients of the considered gases; underestimation was less marked for species larger than methane. The ratio between D_x and D_y components in silicalite-1 was found near one differently from the expected result. The diffusion coefficients obtained using Gusev–Suter approach in silicalite-1 and silica-sodalite can be improved with an appropriate average displacements definition, set in this work equal to 0. Concerning the anisotropy diffusion in silicalite-1, this work shows that correlated jumps in a Gusev–Suter procedure would also be considered. Gusev–Suter computational time for diffusivity estimation of Xe, CF_4, CO_2 and SF_6 is much shorter than the corresponding molecular dynamics (MD) simulation time.

Keywords: Transition-state theory (TST); Diffusion coefficients; Silica-sodalite zeolite

1. Introduction

Zeolites are microporous solids having a large variety of laboratory and industrial applications [1]. They are useful as adsorbents, filters, solid catalysts, and also as membranes for gas separation by controlling gas relative mobility. The understanding of the dynamics fundamentals of small molecules inside a zeolite is relevant for all applications. A certain number of books and articles deal with the important topic of molecular diffusion in zeolite matrices [2,3]. Intra-crystalline zero-loading-diffusion of guest molecules in zeolites

* Corresponding author. Tel.: +39-0984-492-014; fax: +39-0984-402-103.
E-mail address: g.deluca@itm.cnr.it (G. De Luca).

1383-5866/$ – see front matter © 2003 Elsevier B.V. All rights reserved.
doi:10.1016/j.seppur.2003.07.002

can be accurately and successfully reproduced by different computational approaches [4–8].

Gusev–Suter (GS) [9] method is essentially based on the classic transition-state theory (TST) in which the thermal motion of the host matrix is also taken into account. The method is applied to describe the motion of light gases [10,11] in elastic polymeric matrices. In GS procedure, the elastic thermal motions can be estimated by means of a MD simulation of the host matrix [9].

A systematic GS application to gas diffusion in zeolites could be interesting to understand the method timeliness in this field, even if GS calculations are different from the more accurate results of MD and kinetic Monte Carlo (MC) calculations [7,8,12–14]. At the moment, the study on the corrected-diffusivity according to the quantity of adsorbed molecules is not the aim of this work since the accuracy of the starting point, zero-coverage diffusivity, evaluated with GS approach has before established. Previous methods [15] use diffusion coefficients from MD and kinetic MC simulations in the integration of the Fick's law through the membrane. In this work, for mass transport description, a classic model equation is used with the diffusion coefficients derived from GS method.

Reliability and limits of the GS method were studied for the intra-crystalline diffusion of light gases in silicalite-1, zeolite already used also as membrane, and silica-sodalite. Zero-loading-diffusion coefficients of 12 gases at different temperatures were calculated using two force fields, CVFF and CVFF_aug, and a different structural model for each zeolite. The considered gases can be divided in three groups, noble gases (He, Ar, Xe), inorganic molecules (H_2, N_2, O_2, CF_4, CO_2 and SF_6) and light hydrocarbons (CH_4, i-C_4H_{10}). These gases are frequently treated as zeolitic guests in modelling studies [15,16] since various industrial purification processes involve these gases and not only for their relative simplicity. In addition, Theodorou [12] treated Xe and SF_6 molecules in silicalite-1 through a TST procedure with dynamic corrections, whereas Vlugt et al. [13] reported i-C_4H_{10} diffusion considering the species as a combination of connected spheres (i.e. CH, CH_3). These selected gases have low electrostatic moments (except CO_2) and relatively low polarisability (except i-C_4H_{10}). In the considered zeolites, the dispersion-repulsion contribution is predominant with respect to the electrostatic ones due to hydrophobic nature of silicalite-1. Thus, the guest–framework interaction was described using a Lennard–Jonnes potential type. A second point concerns to the shape of the studied gas molecules, since these gases are considered as rigid spheres. Some remarks about no-exactly spherical molecules, H_2, N_2, O_2, i-C_4H_{10} and CO_2, are necessary and will be given at the paragraph 2.3.

Comparison with previous accurate theoretical values from other approaches [7,8,12] and direct measurements of zero-loading-diffusion coefficients (PGF-NMR) [17,18] allows understanding the actual limits and possibilities of the Gusev–Suter approach. In addition, a comparison with experimental data of steady-state gas permeation through a silicalite-1 membrane [19] gives some information on the use of the calculated parameters in non-atomistic (macroscopic) models.

Moreover, the zero-loading-diffusion coefficients for H_2, He and Ne in silica-sodalite were also calculated, since this zeolite has the same chemical composition of silicalite-1 but a different framework structure. In fact, this material has not channels but interconnected sodalite cages.

Computational expense involved in the use of MD techniques for large molecules is considerable. Kinetic MC and TST require substantially less computational effort and in particular GS approach allows taking into account in an easy way also the host matrix vibrations. In addition, until now GS approach was applied only for gas diffusion in polymeric matrix.

Furthermore, zeolite thermal elastic description by means of a smearing vector and its use for any atom type of the host matrix or for atom clusters opens various possibilities to the Gusev–Suter method application.

2. Model and procedure

2.1. The Gusev–Suter approach

Thermally activated particle escaping from a local minimum (site) i to an adjacent site j can be described by the rate constant R_{ij}:

$$R_{ij} = \frac{kT}{h}\frac{Q_{ij}}{Q_i} \tag{1}$$

where k is the Boltzmann constant, h the Planck constant, Q_i and Q_{ij} are the partition functions of guest molecule in the minimum i and in the activated state from site i to site j, respectively. The particle transition probability w_{ij} from site i to a particular adjacent site j is proportional to the rate constant R_{ij}:

$$\omega_{ij} = \tau_i R_{ij} \tag{2}$$

The normalisation constant τ_i, the particle mean life time residing in the site i, is

$$\tau_i = \frac{1}{\sum_j R_{ij}} \tag{3}$$

where the summation is made for all j adjacent sites having common crest surfaces Ω_{ij} with i. These equations lead to a simple procedure for stochastic trajectory simulation of the guest molecules in the host matrix.

The quasi-classical approximation was used for evaluating the partition functions Q_i and Q_{ij}. The partition function of a particle of mass m, localised in the site i, can be written as

$$Q_i = \left(\frac{2\pi mkT}{h^2}\right)^{2/3} \int_{V_i} \mathrm{e}^{-U(\bar{X})/kT}\,\mathrm{d}V \tag{4}$$

where V_i is the volume of the site i and $U(\bar{X})$ is the interaction potential energy between a guest molecule at point $\bar{X}$ and the host matrix atoms. Following the quasi-classical approximation, the guest momentum can be integrated separately from the spatial co-ordinates. The partition function of the activated transition state between sites i and site j is

$$Q_{ij} = \frac{2\pi mkT}{h^2} \int_{\Omega} \mathrm{e}^{-U(\bar{X})/kT}\,\mathrm{d}S \tag{5}$$

where dS denotes the element of the crest surface Ω_{ij}. Putting Eqs. (4) and (5) in Eq. (1) gives

$$R_{ij} = \sqrt{\frac{kT}{2\pi m}} \frac{\int_{\Omega} \mathrm{e}^{-U(\bar{X})/kT}\,\mathrm{d}S}{\int_{V} \mathrm{e}^{-U(\bar{X})/kT}\,\mathrm{d}V} = \sqrt{\frac{kT}{2\pi m}} \frac{Z_{ij}}{Z_i} \tag{6}$$

where Z_i and Z_{ij} are the configurational parts of the partition functions. This equation gives the rate constants for site-to-site transitions in the quasi-classical approximation.

Zeolite elastic motion implies a fluctuation of host atoms around their equilibrium position $\bar{x}_\alpha$, Gusev and Suter introduced the probability density function $W(\Delta_1, \Delta_2, \ldots, \Delta_N)$, with $\Delta_\alpha = \bar{x}_\alpha - \langle \bar{x}_\alpha \rangle$ for describing the elastic fluctuation of the host atoms [9]. In this case, the equilibrium probability density $\rho(\bar{X})$ can be written as

$$\rho(\bar{X}) \propto \int W\{\bar{\Delta}\} \mathrm{e}^{-U(\bar{X},\{\bar{x}\})/kT}\,\mathrm{d}\{\bar{\Delta}\} \tag{7}$$

where $U(\bar{X}, \{\bar{x}\})$ is the interaction potential energy at the position $\bar{X}$. The introduction of the equilibrium density function in Eqs. (4) and (5) gives

$$Q_i = \left(\frac{2\pi mkT}{h^2}\right)^{2/3} \int_{V_i} \rho(\bar{X})\,\mathrm{d}V \tag{8}$$

$$Q_{ij} = \frac{2\pi mkT}{h^2} \int_{\Omega_{ij}} \rho(\bar{X})\,\mathrm{d}S \tag{9}$$

Finally, the rate constant for a jump between two adjacent minima can be written as

$$R_{ij} = \sqrt{\frac{kT}{2\pi m}} \frac{\int_{\Omega_{ij}} \rho(\bar{X})\,\mathrm{d}S}{\int_{V_i} \rho(\bar{X})\,\mathrm{d}V} \tag{10}$$

Hence, the elastic fluctuations of the matrix atoms (W) yields ρ that gives the transition rates R_{ij}. In the Gusev–Suter model, the isotropic elastic motion (Debye's approach [20]) is used to approximate the $W(\Delta_1, \Delta_2, \ldots, \Delta_N)$ function in conjunction with the pair approximation to estimate the potential energy function $U(\bar{X}, \bar{x})$. These coupled approximations make the treatment of the guest dynamics in solids remarkably simple and stimulating for several applications in different solid systems, beyond polymeric matrices.

The quasi-classical approximation is appropriate when energy intervals are very small when compared to kT and the particle is in thermal equilibrium in the sites when the barrier height between the sites i and j is bigger or equal to kT. Thus, the simulation temperature range cannot be freely selected. GS procedure, as implemented in GSnet and GSdif [21] packages, gives different possibilities to define the zeolite elastic fluctuations by setting the average displacement of the matrix atoms. The average displacements can be defined in different ways: (i) fixing displacements for all matrix atoms, (ii) by means of a MD calculation before the TST simulation and (iii) through a self consistent MD calculation along with TST simulation.

2.2. Zeolite structures

The MFI-type silicalite crystal considered in this study is non-polar and virtually contains no aluminium atoms. Perfect lattices, no defect, were the assumptions for the considered zeolites. The lattice parameters reported in the open literature were determined from X-ray diffraction. Lattice parameters were reported as $a = 20.022$ Å, $b = 19.899$ Å and $c = 13.383$ Å in the *Pnma* space group (orthorhombic) [22].

The silicalite structure contains two sets of interconnected pores with a mean diameter of about 5.5 Å. The pores directed along the (0 1 0) axis follow a linear path through the crystal. A second pore set follows a zigzag path with its average along the (1 0 0) axis. Diffusion in the (0 0 1) direction is also possible through a very tortuous sequence of successive displacements along different segments of the interconnected pores. The simulation uses an atomistically detailed microstructure produced by superimposed silicalite-1 unit cells (Fig. 1). The simulation box has dimensions of $a = 40.044$ Å, $b = 39.798$ Å and $c = 40.149$ Å, corresponding to $2 \times 2 \times 3$ superimposed cells.

The silica-sodalite structure was taken from X-ray diffraction analysis [23]. This zeolite has a unit cell composition of $Si_{12}O_{24}$ and a cubic symmetry with a lattice constant $a = b = c = 8.83$ Å, as shown in Fig. 2. In the calculations, 8 unit cells ($2 \times 2 \times 2$) were used realising a simulation box with $a = b = c = 17.66$ Å. Silica-sodalite has no channels, but apertures connecting directly sodalite cages. The largest hexagonal window in the sodalite cage is equal to 6.286 Å, whereas the rhombic one is 4.445 Å. The

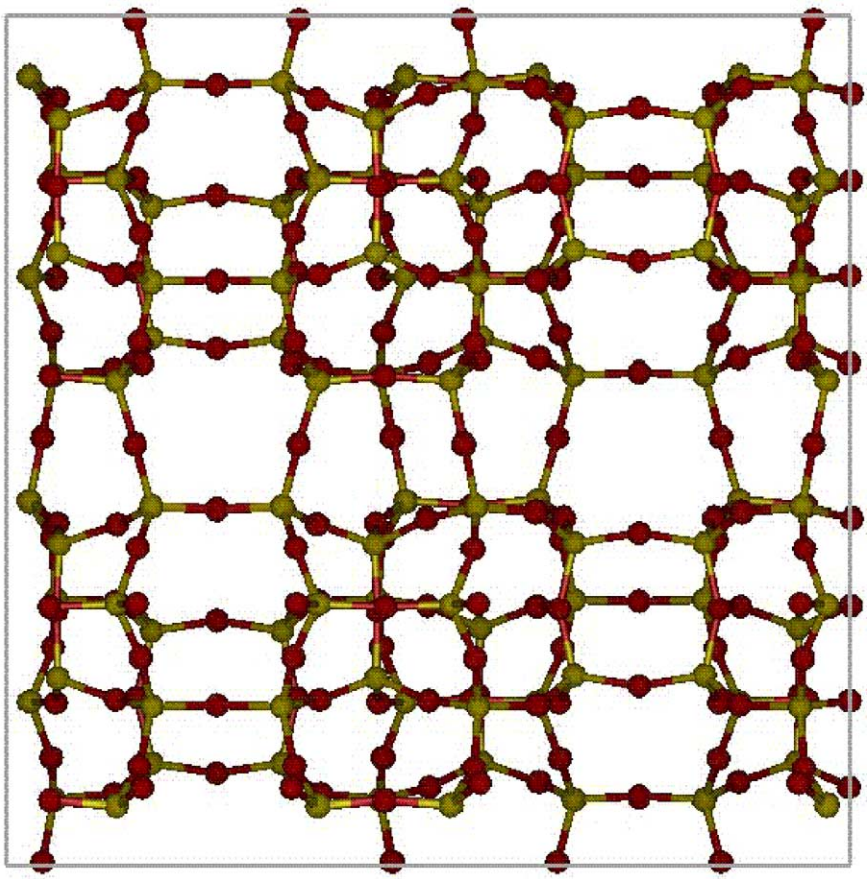

Fig. 1. Unit cell of silicalite-1 zeolite used in atomistic microstructure for simulation volume ($2 \times 2 \times 3$ unit cells) construction. Oxygen and silicon atoms are reported as black and grey, respectively.

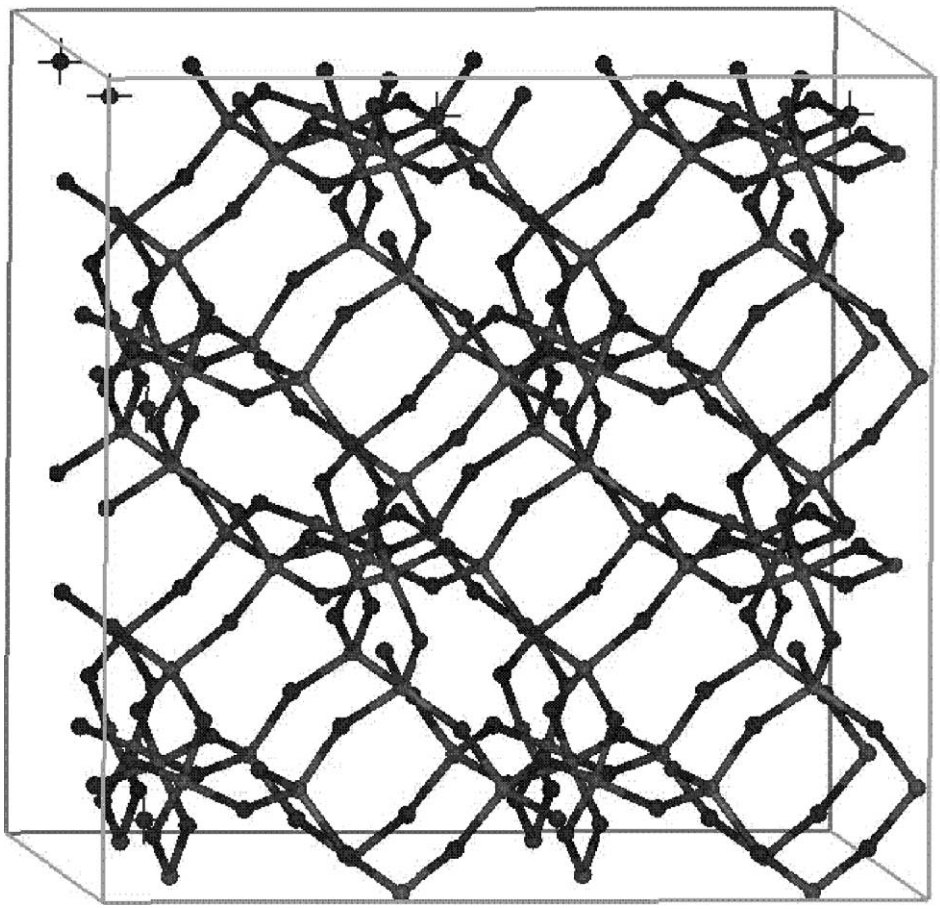

Fig. 2. Unit cell of silica-sodalite zeolite used in simulation box ($2 \times 2 \times 2$ unit cells) construction. Oxygen and silicon atoms are reported as black and grey, respectively.

elasticity introduced by means of a smearing vector is fundamental for the diffusion in this zeolite.

A three-dimensional periodic boundary condition was applied to the simulation cells and all the microstructures were realised with the "Solid Builder of Insight II/Discover" packages of Accelrys [23]. No hydrogen atom was added to the surface of unsaturated oxygen atoms and all the atoms (Si and O) were explicitly treated in Cartesian co-ordinates.

2.3. Potential and dynamics

In the non-polar siliceous species, a simple Lennard–Jones 6–12 function is often used to describe the interaction between the guest particle and the host atoms:

$$U_{\alpha s}(\bar{r}) = -4\varepsilon_{\alpha s}\left[\left(\frac{\sigma_{\alpha s}}{\bar{r}}\right)^6 - \left(\frac{\sigma_{\alpha s}}{\bar{r}}\right)^{12}\right] \tag{11}$$

where $U_{\alpha s}(\bar{r})$ is the interaction potential energy between the guest particle (s) and the host atom type (α) at distance $\bar{r}$. Parameter values of the Lennard–Jones 6–12 interaction between two same guest molecules, σ_{ss} and ε_{ss}, are reported in Table 1. These parameters are commonly used in the study of guest diffusion in rigid zeolites. The Si and O framework parameters ($\sigma_{\alpha\alpha}, \varepsilon_{\alpha\alpha}$) were taken from CVFF and CVFF_aug force fields [21], which were optimised for zeolitic systems. Moreover, the Lennard–Jones potential is truncated at a distance $2(A_{ss}/B_{ss})^{1/6}$, with $A_{ss} = 4\varepsilon_{ss}\sigma_{ss}^{12}$ and

Table 1
Lennard–Jones potential parameters, bond distance and van der Waals radii

Species	σ_{ss} (Å)	ε_{ss} (K)	Reference	Experimental bond distance [24] (Å)	van der Waals radii [25] (Å)	σ_{ss}/d_m
H_2	2.95	37.0	[40]	0.741	1.200	0.94
He	2.56	10.2	[41]	–		
Ne	2.82	32.8	[43]	–		
N_2	3.70	95.0	[40]	1.098	1.500	0.90
O_2	3.46	118.0	[41]	1.207	1.400	0.86
Ar	3.41	120.0	[40]	–		
CH_4	3.82	148.6	[43]	–		
Xe	4.05	231.0	[44]	–		
CF_4	4.34	167.0	[44]	–		
CO_2	3.91	225.3	[42]	1.160 (C–O)	1.40	0.76
i-C_4H_{10}	5.40	300.0	[44]	–	–	1.08[a]
SF_6	5.13	222.1	[43]	–	–	

[a] d_m corresponds to minimum cross-section diameter.

$B_{ss} = 4\varepsilon_{ss}\sigma_{ss}^6$. Interactions between the guest particle and the host atoms were estimated by geometric combination rules. All molecules are treated as the Lennard–Jones single-sphere model (united-atom model) in order to perform the simulation for a reasonably long time and also for large species. However, as mentioned in the introduction, some observations on the spherical shape of H_2, N_2, O_2, CO_2 and i-C_4H_{10} molecules are necessary. The ratio σ_{ss}/d_m near to one is a good indication of the spherical shape. Values equal to 0.94, 0.9, 0.86, 0.76 are obtained for H_2, N_2, O_2, CO_2, respectively, using σ_{ss} reported in Table 1 and d_m calculated as arithmetic mean between the van der Waals radius [24] and the experimental inter-nuclear distance [25]. For i-C_4H_{10} a value of 1.08 was obtained as ratio between σ_{ss} and the minimum cross-section diameter (d_m) (Table 1). These results indicate a satisfactory spherical approximation except for CO_2 molecule. This simple result does not justify the spherical approximation of these species and the non-spherical shape could be taken into account by subsequent corrections, including intra-crystalline partitioning entropy effects [3]. More reliable calculations can be performed with Lennard–Jones parameter for dumbbell molecules for taking into account the non-spherical shape. Finally, the calculation of the $U(\bar{X}, \bar{x})$ potential energy was evaluated at the nodes of equispaced simulation cells with a grid interval of 0.3 Å. With this grid interval, some species (e.g. H_2, He) show a number of potential energy minima higher than the number allowed by the software (600). This effect is not only a software limit; in fact, the species presenting too high minima have also low activation energy. The control on the site number and related energies appear as an important factor for the calculation accuracy in a TST calculation for species (Table 1) with low activation energy. GSnet and GSdif codes [21], based on the original Gusev–Suter approach, were used in the calculations. In particular, GSnet computes the free energy, identifies sites and transition probabilities, whereas GSdif performs a Monte Carlo simulation of gas diffusion by a 'hopping' mechanism using the results supplied by GSnet. Finally, guest zero-loading-diffusivities were computed from the trajectories created by TST–MC simulations from the Einstein relationship:

$$D = \frac{\langle r^2(t)\rangle}{6t} \tag{12}$$

where $\langle r^2(t)\rangle$ is the mean displacement vector at time t and the average is computed over different guest trajectories. The mean-square displacement in the generic co-ordinate at time t is given by

$$\langle X^2(t)\rangle = \frac{1}{N_{\text{trajectories}}} \sum_{i}^{N_{\text{trajectories}}} (X_i(t_0 + t) - X_i(t_0))^2 \tag{13}$$

where t_0 represents the simulation starting time. Every jump is associated with the time increment $\Delta t =$

τ_i (for τ_i see Eq. (3)). Finally, a log ($\langle r^2(t)\rangle$) versus log(t) plot determines if the limiting slope of 1.0 was achieved, thus the true diffusive behaviour was reached in the simulation. Gusev et al. [26] report other computational details such as extent sites, the crest surfaces between them and appropriate values of the surface element.

3. Results and discussion

Inter-atomic parameters, from the open literature (Table 1), are the more common used in zeolite calculations. No parameter adjusting was performed in the present simulations. The average of the mean displacement vector for each species was performed over 2000 different independent trajectories. The simulation time was 10^{-6} s, although a shorter time interval could be used.

Zero-loading-diffusivity of 11 gases calculated by means of GS method using CVFF and CVFF_aug force fields are shown in Table 2. GS approach systematically underestimates the diffusion coefficients with respect to the estimation obtained with more elaborated MD calculations and the more recent kinetic MC [14]. However, this gap is less dramatic for particles like Xe, CF_4 and SF_6. For CH_4 and Ar TST (GS approach) values are more distant from PFG-NMR experimental data [17,18] than the respective MD results. Experimental values refer to 2–4 adsorbed gas particles per unit cell, thus experimental zero-loading-diffusivity is expected to be larger than that reported in Table 2. However, zero-loading-diffusion coefficient estimation in one order of magnitude aims this work. TST (GS approach) results, e.g. for CF_4 and CO_2, were in good agreement with the experimental data reported in Table 2, more than one order of magnitude.

MD coefficients obtained with single simulation run and short dynamics [27] were markedly lower than MD values calculated with 20 simulation runs and long dynamics [7]. The MD values reported by Jost et al. [8] have a good agreement with those of Skoulidas and Sholl and for Xe the results of this work agree too. Less positive result concerns with the ratio between D_x, D_y and D_z components. Thus, the ratio D_x/D_y is incorrect, i.e. all molecules reported in Table 2 prefer switching channel type during the movement through a channel intersection. An analysis of this result and average zero-loading-diffusion values (Table 2) requires different considerations about correlated hops, oscillating framework, dynamical correction, Lennard–Jones parameters and related activation energies. A qualitative analysis of these possible causes will be given at the suitable moment.

As suggested by Murphy et al. [28,29], for a correlated random walk of N elementary steps, δ, the multistate dynamical correction to TST implies that

$$D = D_{\mathrm{GS}}^{xz}\frac{1+\langle\cos\gamma\rangle}{1-\langle\cos\gamma\rangle} \tag{14}$$

where γ is the angle between the path of two consecutive jumps and $D_{GS}^{xz} = \delta^{xz}/6t$ represents the diffusion coefficient of GS method. However, this approach requires MD simulation for the correction factor evaluation to D_{GS} for each studied particle; at qualitative level, the angle between two consecutive segments in the zigzag channel is equal to 1.966 radiant at the channel intersection of the silicalite-1. Therefore, the correction factor $((1+\langle\cos\gamma\rangle)/(1-\langle\cos\gamma\rangle))$ equal to 0.444 reduces the D_x^{xz} components as expected.

Zeolite oscillations do not affect equally the diffusion coefficient components of methane. In particular, Suffritti and co-workers [30] report (D_x, D_y, D_z) equal to (3.59, 14.9, 1.22) $\times$ 10^{-5} cm^2/s and (4.93, 9.66, 1.64) $\times$ 10^{-5} cm^2/s for an oscillating and a rigid framework, respectively.

For an oscillating framework, D_y increases of 5.24 $\times$ 10^{-5} cm^2/s, while D_x decreases of 1.34 $\times$ 10^{-5} cm^2/s with respect to a rigid framework (D_z component remains almost unchanged). The results in Table 2 were obtained with a completely rigid framework. If the variations are in the direction foresaw by Suffritti and co-workers [30], calculation performed with an appropriate smearing vector which takes into account the lattice vibrations can give better absolute diffusion coefficients and relative ratio. Concerning this, it is important to distinguish between the absolute values of the D_x, D_y and D_z components and their relative ratio. In particular, GS average diffusion coefficients (D) are systematically underestimates with respect to the more precise MD calculations and the hierarchy between D_x and D_y values is not correct. A separate analysis of the possible corrections to improve the D_x, D_y and D_z absolute values and the relative ratio were made. It is possible to use a

Table 2
GS, previous MD, kinetic MC, TST calculated and PFG-NMR experimental zero-loading-diffusivity (10^{-5} cm^2/s) for silicalite-1 at 300 K

Species	GS (CVFF_aug)				GS (CVFF)				Previous MD Calculations, D						Kinetic MC and previous TST calculations, D		PFG-NMR
	D_x	D_y	D_z	D	D_x	D_y	D_z	D									
He	[a]	[a]	[a]	[a]	[a]	[a]	[a]	[a]	65.8	66.1							
H_2	[a]	[a]	[a]	[a]	[a]	[a]	[a]	[a]									
O_2	1.42	1.50	0.34	3.26	2.12	2.54	0.54	5.20									
N_2	1.29	1.27	0.83	2.84	2.58	2.70	0.61	5.89				16.0, 25.0					
Ar	1.30	1.27	0.31	2.88	2.00	2.26	0.44	4.70	13.2	6.5							
CH_4	1.12	1.10	0.26	2.48	2.57	2.84	0.62	6.04	14.5	3.9	10.0		13.4	14.0	15.0		>10[b], 7[c]
Xe	0.13	0.15	0.03	0.31	0.53	0.59	0.13	1.26	2.3	1.0	1.8		1.86				4[d]
CF_4	0.08	0.08	0.02	0.18	1.04	1.14	0.22	2.40	4.5						3.0		2.5[e]
CO_2	0.38	0.40	0.09	0.87	1.00	1.12	0.23	2.30				9.5, 7.0					2.4[f] 2.8[g]
SF_6	[h]	[h]	[h]	[h]	0.21	0.22	0.05	0.48	0.5							0.36, 0.26	
i-C_4H_{10}	[h]	[h]	[h]	[h]	0.02	0.03	0.00	0.05									
Reference									[7]	[27]	[8]	[37]	[31,45]	[12]	[14]	[13]	

The calculations were made using CVFF_aug and CVFF force fields and for a simulation box ($2 \times 2 \times 3$ unit cells) with dimension of 40.044 Å × 39.798 Å × 40.149 Å.

[a] Too many minima (see text).

[b] [17].

[c] [18].

[d] [12].

[e] [32].

[f] [38].

[g] [39].

[h] No convergence (convergence condition $(\mathrm{d}\log\langle r^2\rangle/\mathrm{d}\log(t)) = 1$).

smearing vector different from zero to increase simultaneously all D_x, D_y and D_z values, and a correction factor in Eq. (14) to reduce only the D_x values with respect D_y. However, an underestimation is still more evident if the correction factor is not-coupled with a smearing factor.

A previous calculation made by Theodorou and co-workers [13] on SF_6 and Xe shows that the dynamic correction on TST values should be taken into account. In particular, D values of 0.36 and 0.26 with and without dynamic correction, respectively (Table 2) were reported for SF_6 by Theodorou and co-workers [13]. Eq. (1) is only an approximation and ignores detailed system dynamics. In particular, the average effect of the "bath" can be imposed through an effective friction factor. The non-reactive re-crossing of the transition state is the dynamics feature missed by TST. A phenomenological correction to TST can be used, in which a great deal of dynamical information is included into a transmission factor, here assumed equal to 1.

Finally, to understand the systematic underestimation of the results reported in Table 2 it is necessary to take into account Lennard–Jones parameters, which characterise the guest–host interactions and the related diffusion activation energies. The used potential takes explicitly into account silicon atoms, whereas in MD and MC works these atoms are considered by means of opportune parameters of the oxygen atoms of the zeolite. In particular, for methane Goodbody et al. [31] introduced (CH_4–O_z) MD parameters obtained by the experimental Henry constant fitting. This aspect could contribute furthermore to the underestimation of GS values.

In the kinetic MC simulation of Paschek and Krishna [14], the equation defining the mean life time is similar to Eq. (3) and that defining the probability of a single particle jump is similar to Eq. (2). They used an equal-spaced site lattice which can be occupied by only one particle at the same time, these lattice sites do not represent exactly the minima of the adsorbed particles potential energy surface. Periodic boundary conditions are used in the simulations. The transition probabilities used by Paschek and Krishna [14], determined by rate constants (see Eq. (2)), were defined to match the MD zero-loading-diffusion values of Goodbody et al. [31] and Snurr and Kärger [32]. Moreover, the methane activation energy of the rate constant were settled by Paschek and Krishna to be almost 4.2 kJ/mol (1 kcal/mol) for fitting the temperature dependence of the experimental and MD simulation diffusivity data of Snurr and Kärger [32]. Similarly to Paschek and Krishna [14], this work could have defined a potential of molecule–zeolite interaction or a smearing factor for reproducing the activation energies obtained experimentally or through MD calculations. However, this work is aimed to establish the accuracy level of a GS approach in zeolitic systems.

Moreover, H_2 and He present a number of minima higher than the limit allowed by the GSNet package (600). In any case, configurational part of the partition functions for He and H_2 (see Eq. (6)) is less important than the part related with the mean speed (σ_{ss} and ε_{ss} values are the smallest of those reported in Table 1). Better results should be expected if the mean speed is calculated using MD rather than the thermal equilibrium as suggested by Murphy et al. [29]. GS approach seems to represent a starting point for the diffusion coefficient evaluation even though systematically less accurate than MD.

Zero-loading-diffusion coefficients fitted by Bakker et al. [19] using experimental data measured by gas diffusion in silicalite-1 membrane were used for comparison with GS results (Table 3). Bakker et al. [19] proposed two different diffusion regimes for silicalite-1 membrane depending on the temperature: at low temperature, surface diffusion takes places, and at high temperature gas translation diffusion occurs. A given temperature and loading, they assumed both diffusion mechanisms contribution to the overall mass transport through the silicalite-1. Gas translation diffusion, e.g. at 300 K is almost zero. It is important to underline that the Bakker et al. [19] model considers only the diffusion in zeolitic pores (intra-crystalline diffusion). They defined the total permeating flux through the zeolite membrane as

$$J|_{dx} = -\varepsilon \left[\left(\rho q_{sat} D_s^0(\theta = 0) e^{-E_{DS}/RT} \frac{1}{1-\theta} \right) \frac{d\theta}{dx} + \left(\frac{\lambda}{z} \sqrt{\frac{8}{\pi MRT}} e^{-E_{DGT}/RT} \right) \frac{dP}{dx} \right] \quad (15)$$

where ε is the porosity of metal–support layer, ρ the silicalite-1 density, whereas q_{sat} is the saturation

Table 3
GS calculated zero-loading-diffusivity (10^{-5} cm^2/s) and experimental (in membrane) diffusion coefficients for silicalite-1 at 300 K

Species	D			$D_{CVFF\text{-}aug}/D_{exp}$	D_{CVFF}/D_{exp}
	CVFF_aug	CVFF	Bakker et al. [19]		
O_2	3.26	5.20	–		
N_2	2.84	5.89	1.47	1.93	4.00
Ar	2.88	4.70	2.72	1.05	1.72
CH_4	2.48	6.04	1.19, 3.0[a]	2.08, 0.83	5.07, 2.01
Xe	0.31	1.26	0.24	1.29	5.25
CO_2	0.87	2.30	0.16	5.43	14.37
CF_4	0.18	2.40	–		
i-C_4H_{10}	–	0.05	0.004		
SF_6	–	0.48	0.01		

The calculations were made using CVFF_aug and CVFF force fields and for a simulation box (2 × 2 × 3 unit cells) with dimension of 40.044 Å × 39.798 Å × 40.149 Å.
[a] [46].

capacity and z is a probability factor (for silicalite-1 it is equal to four). The occupancy θ is a function of the temperature given by the Langmuir isotherm.

Eq. (15) presents four unknown parameters, $D_s^0(0)$, E_{DS}, λ and E_{DGT}. The equilibrium parameters, necessary to define θ, were obtained from independent measurements of the adsorbed amount versus the temperature (isobar at 101 kPa). These parameters were varied to reproduce the experimental total flux through silicalite-1 membrane. Rewriting Eq. (15) as

$$J|_{dx} = -\varepsilon\left[\left(\rho q_{sat} D_s^0(\theta=0)e^{-E_{DS}/RT}\frac{1}{1-\theta}\right) \times \frac{b(1-\theta)^2}{1-2\theta} + \left(\frac{\lambda}{z}\sqrt{\frac{8}{\pi MRT}}e^{-E_{DGT}/RT}\right)\right]\frac{dP}{dx} \quad (16)$$

where $b(1-\theta)^2/(1-2\theta)$ is the derivative of the Langmuir monosite isotherm $\theta = bP/(1+bP)$.

Assuming a weak θ change with pressure, the integrated form over the whole silicalite-1 membrane thickness (δ) is

$$J|_{\delta} = -\varepsilon\left[\left(\rho q_{sat} D_s^0(\theta=0)e^{-E_{DS}/RT}\frac{1}{1-\theta}\right) \times \frac{b(1-\theta)^2}{1-2\theta} + \left(\frac{\lambda}{z}\sqrt{\frac{8}{\pi MRT}}e^{-E_{DGT}/RT}\right)\right]\frac{\Delta P}{\delta} \quad (17)$$

and the permeance results:

$$\text{Permeance} = \frac{J|_{\delta}}{\Delta P} = -\varepsilon\left[\left(\rho q_{sat} D_s^0(\theta=0)e^{-E_{DS}/RT}\frac{1}{1-\theta}\right) \times \frac{b(1-\theta)^2}{1-2\theta} + \left(\frac{\lambda}{z}\sqrt{\frac{8}{\pi MRT}}e^{-E_{DGT}/RT}\right)\right]\frac{1}{\delta} \quad (18)$$

From Eq. (18) it can be noted that the ratio between experimental diffusivity at zero coverage, $D_s^0(\theta = 0)e^{-E_{DS}/RT}$, and computed zero-loading-diffusivity is proportional to the ratio between the experimental and theoretical permeation when the gas translation diffusion is negligible.

Table 3 reports the ratio between fitted $D_s^0(\theta = 0)e^{-E_{DS}/RT}$ and GS calculated diffusivity. Diffusion coefficients were divided in three different groups. In particular, CVFF_aug force field gave the best agreement with the experimental data on membrane measurements [19] and CVFF results were relatively nearer with respect to CVFF_aug to PGF-NMR data [17,18] and MD simulations [7,8,12] (Table 2). Diffusion coefficients of some species (e.g. CH_4) measured with methods based on membrane (square wave) [33], quasi steady-state single-crystal permeation [34] and Bakker et al. [19], agree reasonably among them

but they differ by orders of magnitude from that measured with microscopic methods [17,18,35,36] (Table 2). Agreement between membrane permeation, MD and GS results is satisfactory for Xe, while SF_6 agrees well with MD calculations, but not at all with membrane measurements. These results confirm that every species should be considered individually and their trends should be treated with caution. For both force fields, when σ_{ss} approaches to the pore diameter of silicalite-1 membrane, GS method is less reliable when compared with Bakker et al. fitting [19], whereas it gives better results with respect MD calculations. Molecules with σ greater than 5.0 Å did not converge using CVFF_aug force field because, probably, no smearing vector was used. Therefore, a vector definition with values different from zero could be interesting, although more detailed studies should be necessary. From Table 3, a diffusion coefficient overestimation can be observed, in particular for CO_2, SF_6 and *i*-C_4H_{10}. There is a difference of one order of magnitude between microscopic measurements and membrane measurements and GS values underestimate the microscopic data and overestimate the membrane ones. Concerning these differences, Bakker et al. model [19] takes into account only the intra-crystalline surface and gas transport diffusion and does not consider any membrane defect.

Table 2 gives a direct comparison between GS results and those of other theoretical procedures together with specific measures of the zero-loading-diffusion coefficients. Table 3 gives a measure of how the TST approximation on single crystal can be available or not with respect to a macroscopic membrane model. As far as this subject is concerned, it is important to observe the results obtained for the CO_2. Equilibrium dynamic values for CO_2 were taken from the recent work of Makarodimitris et al. [37]. The authors modelled CO_2 molecule as two consecutive dumbbells sharing the central carbon atom, arranged on a straight line, while N_2 was modelled as a single dumbbell with a rigid inter-atomic bond. In Table 2, two values of zero-loading-diffusion coefficients were reported, since Makarodimitris et al. [37] use two different models in conjunction with two different zeolite models for each species (N_2 and CO_2). These zeolite models differ for the presence or absence of partial charges on zeolite oxygen and on the Lennard–Jones parameters (see paragraph 4.4 of [37]). In the case of N_2 the difference between the two models, even using the same procedure (equilibrium molecular dynamics) is of 10×10^{-5} cm^2/s, whereas for CO_2, it is of 2×10^{-5} cm^2/s. The difference between this work and Makarodimitris et al. [37] values are from 10 to 20×10^{-5} cm^2/s, taking into account the approximation adopted in the GS calculations, the result is satisfactory. Although the CO_2 no-perfectly spherical shape, a comparison of the present results with PFG-NMR [38], frequency response [39] and fitting on flux in silicalite-1 membranes [19] (Table 3), respectively, shows that the analyses done for the other species are still valid for CO_2.

A good theoretical result (MD, TST, kinetic MC) when compared to an experimental direct measurement of the diffusion coefficients may not be a good parameter for Eq. (18). In fact, the comparison between the $D_s^0(\theta = 0)e^{-E_{DS}/RT}$ obtained in the present work and the previous theoretical and experimental results (Table 2) puts into light some deceptive results. For some species (Ar, CH_4, N_2) the parameters calculated using GS approach for a mono-crystal with periodic boundary condition are satisfactory when compared with membrane fitting results [19] (Table 3), but there is a significant discrepancy with direct measurements of zero-loading-diffusivities. As underlined with the model used by Bakker et al. [19], this difference depends on the chosen atomistic model and related non-atomistic equation.

In Fig. 3, the mean square displacements of Xe computed with CVFF_aug force fields versus simulation time are presented. The behaviour of the other studied gases is similar to Xe atom. Finally in Fig. 4, the mean square displacements of CH_4, N_2 and Xe versus time are presented in logarithmic scale. The linearity is already achieved to 10^{-11} s. In all cases, the simulation time used is larger than necessary. In any case, a very short computational time is required by Gusev–Suter method for 10^{-6} s of simulation. As suggested by Gusev et al. [26], it is important to take care of the ratio between the simulation box dimensions and simulation times, even when periodic boundary conditions are present. Other studies on this ratio are in progress.

Table 4 presents D_y component of zero-loading-diffusivity computed in a simulation volume corresponding to $2 \times 2 \times 3$ superimposed silicalite-1 unit cells and in cubic simulation box with dimension $a = b = c = 20$ Å. Attention has to be paid on this last

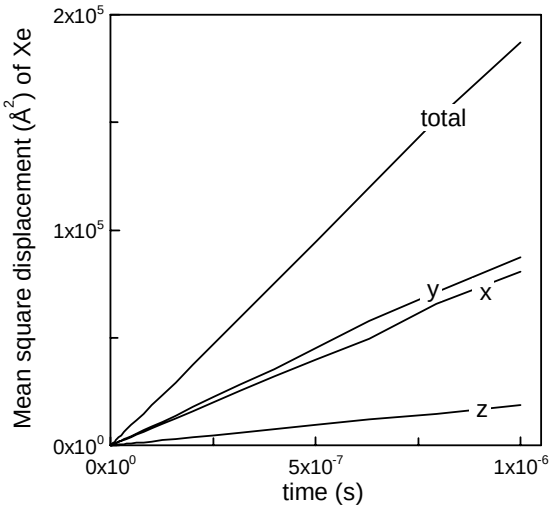

Fig. 3. Mean square displacement of Xe vs. the simulation time for silicalite-1 zeolite. The computation proceeded up to 10^{-6} s and the averages were performed over 2000 different independent trajectories. CVFF_aug force field was applied to a simulation box of $2 \times 2 \times 3$ unit cells.

box, in fact the crystallographic silicalite-1 parameters used in this work are $a = 20.022$ Å, $b = 19.899$ Å and $c = 13.383$ Å. Therefore, the perfectly cubic box results almost one and a half larger of the crystallographic unit cell. A silicalite-1 unit cell was arbitrarily cut in the *XY* plane, leaving unchanged the *Y* component and applying the periodic boundary conditions. It is not strange that with this arbitrary cutting the only *Y* component must remain constant as shown in Table 4.

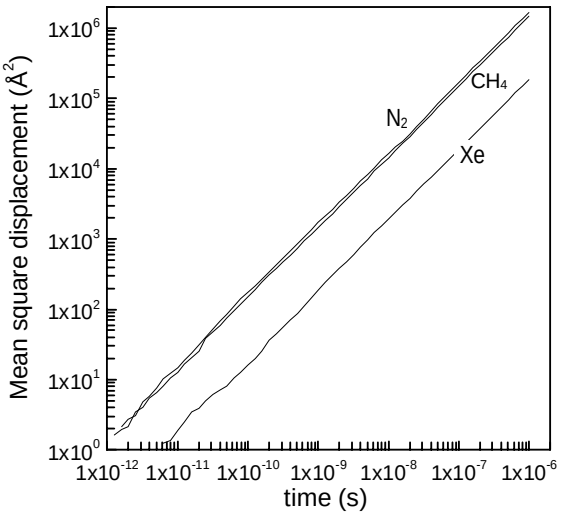

Fig. 4. Mean square displacement for CH_4, N_2 and Xe vs. the simulation time for silicalite-1 zeolite. The computation proceeded up to 10^{-6} s and the averages were performed over 2,000 different independent trajectories. CVFF_aug force field was applied to a simulation box of $2 \times 2 \times 3$ unit cells.

Table 4
D_y zero-loading-diffusivity computed in $2 \times 2 \times 3$ superimposed silicalite-1 unit cells and a cubic simulation volume

Species	D_y ($\times 10^{-5}$ cm^2/s)			
	$2 \times 2 \times 3$ superimposed unit cells		Cubic simulation volume	
	CVFF_aug	CVFF	CVFF_aug	CVFF
He	[a]	[a]	6.21	15.85
H_2	[a]	[a]	8.35	17.71
N_2	1.27	2.70	1.20	2.40
O_2	1.50	2.54	1.43	2.40
Ar	1.27	2.26	1.26	1.80
CH_4	1.10	2.84	1.10	2.50
Xe	0.15	0.59	0.15	0.50
CF_4	0.08	1.14	0.09	0.90
CO_2	0.40	1.12	0.42	0.90
SF_6	[b]	0.22	[b]	0.22
i-C_4H_{10}	[b]	0.03	[b]	0.04

The calculations were made with CVFF_aug and CVFF force fields at 300 K.
[a] Too many minima (see text).
[b] No convergence (convergence condition $(d \log\langle r^2\rangle / d \log(t)) = 1$.

Murphy et al. [29] calculated single guest diffusion for the noble gases through silica-sodalite zeolite using a classical TST. Full MD calculation and classical diffusivities for He were compared. Therefore, the Gusev–Suter method performance is also tested for this species in the same zeolite. Table 5 presents diffusion coefficients, at 300 K, for H_2, He and Ne with CVFF force field in the cubic cell of silica-sodalite described in the previous section 2.2. In this case, a smearing vector module equal to 1.5 Å was necessary in order to obtain the convergence for all three species. The smearing vector was fitted to reproduce (the order of magnitude) the Murphy et al. [29] diffusion coefficient for He atom. This vector was used for the other guest species. The analysis of Table 4 shows that the same smearing vector for Ne does not reproduce the values obtained by Murphy et al. [29]. Contrary of silicalite-1, for silica-sodalite a smearing factor, at the same temperature, was necessary for obtaining the

Table 5
GS zero-loading-diffusion coefficients, TST and MD diffusion coefficients from Murphy et al. [29]

Species	Zero-loading-diffusion coefficients ($\times 10^{-5}$ cm^2/s)						τ_{GS} (ps)	τ_{TST} (ps)
	GS				TST	MD		
	D_x	D_y	D_z	D				
H_2	0.50	0.52	0.52	1.54			67	
He	1.77	1.77	1.66	5.20	4.3	3.8	19	23
Ne	0.24	0.24	0.23	0.71	7.1×10^{-4}		140	14×10^4
Reference					[29]	[29]		

Cage residency times (τ) for hydrogen and noble gases in silica-sodalite.

result convergence. It is important to emphasise that this factor is directly correlated with the zeolite elastic motion. The smearing vector used here may mask the dynamic corrections and other effects previously discussed. Therefore, further studies are desirable before its introduction. Gusev–Suter approach indicates that He is trapped in sodalite cages (at room temperature) for a time of the order of 20 ps, result in good agreement with previous TST and MD calculations. Explicitly, Ne dynamics simulation (at room temperature) is hence computationally expensive and then demonstrates the utility of a GS approach in this case.

An appropriate smearing factor is an important parameter in a GS calculation for silicalite-1. However, for silica-sodalite this parameter becomes fundamental to obtain a diffusion coefficient different from zero with GS approach. Silica-sodalite presents only sodalite cages connected directly by hexagonal and rhombic windows; thus for a completely rigid structure, the jumps between the cages through the window is extremely unlikely as shown recently by Murphy et al. [29]. Therefore, GS calculations need a smearing vector different from zero to calculate the diffusivity in silica-sodalite, unlike the silicalite-1 system.

4. Conclusions

GS method was applied to evaluate zero-loading-diffusion coefficients in silicalite-1 and in silica-sodalite using CVFF_aug and CVFF force fields.

Diffusion coefficient of 12 gases (He, Ne, Ar, Xe, H_2, N_2, O_2, CO_2, SF_6, CH_4, CF_4, and *i*-C_4H_{10}) in silicalite-1, and zero-loading-diffusion coefficients for H_2, He, Ne, in silica-sodalite, were calculated. A comparison with previous TST, MD and also kinetic MC values was presented.

The results for silicalite-1 can be summarised: (i) GS values systematically underestimate the accurate MD results and PGF-NMR data, (ii) the ratios between D_x and D_y diffusion coefficients are different from the expected values for the same zeolite.

For silica-sodalite a smearing vector different from zero is necessary for the simulation convergence.

In the light of these results, some corrections were suggested and justified. In particular, for silicalite-1 the use of appropriate smearing factor is highly recommendable for result improving, moreover dynamic correction and different Lennard–Jones parameters were also suggested.

GS procedure is attractive for its simplicity in taking into account the zeolitic structure actual distortions at different temperatures. However, this work represents a starting point for diffusion coefficient evaluation.

Finally, other force fields, taking into account other energetic contributes like electrostatic ones, are also desirable to extend the method to the zeolites containing cations.

References

[1] F. Ribeiro Ramoa, et al. (Eds.), Zeolites: Science and Technology, Nijhoff, Boston, 1984.
[2] J. Kärger, D.M. Ruthven, Diffusion in Zeolites and Other Microporous Solids, Wiley, New York, 1992;
N.Y. Chen, et al., Molecular Transport and Reaction in Zeolites, VCH, New York, 1994.
[3] J. Xiao, J. Wei, J. Chem. Eng. Sci. 47 (1992) 1123–1143.

[4] R.L. June, A.T. Bell, D.N. Theodorou, J. Phys. Chem. 96 (1992) 1051.
[5] F. Jousse, D.P. Vercauteren, S.M. Auerbach, J. Phys. Chem. B 104 (2000) 8768–8778.
[6] H. Takaba, A. Koyama, S. Nakao, J. Phys. Chem. B 104 (2000) 6353–6359.
[7] A.I. Skoulidas, D.S. Sholl, J. Phys. Chem. B 106 (2002) 5058–5067.
[8] S. Jost, N. Bar, S. Fritzsche, R. Haberlandt, J. Kärger, J. Phys. Chem. B 102 (1998) 6375.
[9] A.A. Gusev, U.W. Suter, J. Chem. Phys. 99 (3) (1993) 2228.
[10] A.A. Gusev, U.W. Suter, J. Comput. Aided Mater. Design 1 (1993) 63–73.
[11] M. Heuchel, D. Hofmann, Desalination 144 (2002) 67–72.
[12] R.L. June, A.T. Bell, D.N. Theodorou, J. Phys. Chem. 94 (1990) 8232–8240;
R.L. June, A.T. Bell, D. N Theodorou, J. Phys. Chem. 97 (1993) 4173–4181.
[13] R.L. June, A.T. Bell, D.N. Theodorou, J. Phys. Chem. 95 (1991) 8866;
T.J.H. Vlugt, C. Dellago, B. Smit, J. Chem. Phys. 113 (2000) 8791.
[14] D. Paschek, R. Krishna, Langmuir 17 (2001) 247–254.
[15] T.C. Bowen, J.L. Falconer, R.D. Noble, A.I. Skoulidas, D.S. Sholl, Ind. Eng. Chem. Res. 41 (2002) 1641–1650.
[16] R. Nagumo, H. Takaba, S. Suzuki, S. Nakao, Micropor. Mesopor. Mater. 48 (2001) 247–254.
[17] J. Caro, M. Bulow, W. Schirmer, J. Karger, W. Heink, H. Pfeifer, S.J. Zdanov, J. Chem. Soc., Faraday Trans. 81 (1985) 2541–2550.
[18] J. Karger, W. Krause, H.Z. Pfeifer, Phys. Chem. (Leipzing) 264 (1985) 838.
[19] W.J.W. Bakker, L.J.P. van den Broeke, F. Kapteijn, J.A. Moulijn, AIChE J. 43 (1997) 2203.
[20] P. Debye, Verh. Deut. Physik. Ges. 15 (1913) 783.
[21] Discover User Guide, Version 4.0.0, Accelrys, San Diego, 1996.
[22] D.H. Olson, G.T. Kokotailo, S.L. Lawton, W.M. Meier, J. Chem. Phys. 85 (1981) 2238.
[23] Catalysis User Guide, Solid Builder Section, Version 4.0.0, Accelrys, San Diego, 1996.
[24] A. Bondi, J. Phys. Chem. 68 (3) (1964) 441.
[25] D.R. Lidd, CRC Handbook of Chemistry and Physics, 76th ed., CRC Press, Boca Raton, FL, 1995–1996.
[26] A.A. Gusev, A. Simone, U.W. Suter, D.J. Moll, J. Chem. Phys. 99 (3) (1993) 2221.
[27] S. Kar, C. Chakravarty, J. Phys. Chem. A 105 (2001) 5785–5793.
[28] A.F. Voter, J.D. Doll, J. Chem. Phys. 82 (1985) 80.
[29] M.J. Murphy, J.A. Voth, A.L.R. Bug, J. Phys. Chem. B 101 (1997) 491–503.
[30] P. Demontis, E.S. Fois, G.B. Suffritti, J. Phys. Chem. 94 (1990) 4329–4334.
[31] S.J. Goodbody, K. Watanabe, D. MacGowan, J.P.R.B. Walton, N. Quirke, J. Chem. Soc., Faraday Trans. 87 (13) (1991) 1951–1958.
[32] R.Q. Snurr, J. Kärger, J. Phys. Chem. B 101 (1997) 6469.
[33] D. Shen, L.V.C. Rees, J. Caro, M. Bulow, B. Zibrowius, J. Chem. Soc., Faraday Trans. 86 (1990) 3943.
[34] D.B. Shah, S. Chokchai-Acha, D.T. Hayhurst, J. Chem. Soc., Faraday Trans. 89 (1993) 3161.
[35] W. Heink, J. Kärger, H. Pfeifer, K.P. Datema, A.K. Nowak, J. Chem. Soc., Faraday Trans. 88 (1992) 3505.
[36] H. Jobic, M. Bee, J. Caro, in: R. von Ballmoos, J.B. Higgins, M.J. Treacy (Eds.), Proceedings of the 9th International Zeolite Conference, vol.2, Butterworth-Heinemann, Stoneham, 1993, p. 121.
[37] K. Makarodimitris, G.K. Papadopoulos, D.N. Theodorou, J. Phys. Chem. B (2001) 105, 777–788.
[38] J. Kärger, H. Pfeifer, F. Stallmach, N.N. Feoktistova, S.P. Zhdanov, Zeolites 13 (1993) 50.
[39] D. Shen, L.J. Rees, J. Chem. Soc., Faraday Trans. 90 (1994) 3011.
[40] G.C. Maitland, M. Rigby, E.B. Smith, W.A Wakehan, Intermolecular Forces, Clarendon Press, Oxford, 1981.
[41] A.B. Shelekhin, A.G. Dixon, Y.H. Ma, AIChE J. 41 (1) (1995) 58.
[42] J.J. Nicolas, K.E. Gubbins, W.B. Streett, D.J. Tildesley, Mol. Phys. 37 (1979) 1429–1454.
[43] W.A. Steele, The Interaction of Gases with Solid Surfaces, Pergamon Press, Oxford, 1974.
[44] R.C. Reid, J.M. Prausnitz, T.K. Sherwood, The Properties of Gases and Liquids, McGraw-Hill, New York, 1977.
[45] S.D. Pickett, A.K. Nowak, J.M. Thomas, B.K. Peterson, J.F.P. Swift, A.K. Cheetham, C.J.J. den Ouden, B. Smit, M.F.M. Post, J. Phys. Chem. 94 (1990) 1233.
[46] F. Kapteyn, W.J.W. Bakker, G. Zheng, J. Poppe, J.A. Moulijn, Chem. Eng. J. 57 (1995) 145–153.